Published in Intermetallics, Vol. 31, pp.55-64 (2012).
http://dx.doi.org/10.1016/j.intermet.2012.06.010

The crystal structure of the LPSO phase of the 14*H* type in the Mg-Al-Gd alloy system

K. Kishida[1,*], H. Yokobayashi[1], H. Inui[1], M. Yamasaki[2] and Y. Kawamura[2]
[1] Department of Materials Science and Engineering, Kyoto University,
Sakyo-ku, Kyoto, 606-8501 JAPAN
[2]Department of Materials Science, Kumamoto University
2-39-1, Kurokami, Kumamoto 860-8555, JAPAN

Abstract

The crystal structure of a long-period stacking-ordered (LPSO) phase of the 14*H* type formed in a Mg-Al-Gd alloy as a local small part in the intergrowth structure together with that of the 18*R* type (the majority) has been investigated by scanning transmission and transmission electron microscopy. The LPSO phase of the 14*H* type in the Mg-Al-Gd system is found to form by stacking structural blocks, each of which consists of seven close-packed atomic planes. In each of structural blocks, a long-range ordering occurs for the constituent Mg, Al and Gd atoms with the enrichment of Gd atoms in the four consecutive atomic planes. The in-plane long-range ordering in the four consecutive atomic planes occurs so as to form Al_6Gd_8 clusters in a periodic manner. This is exactly the same as what is observed in the LPSO phase of the 18*R* type. The crystal structure of the 14*H*-type LPSO phase can thus be described to form simply by adding a Mg layer to the crystal structure of the 18*R*-type LPSO phase so as to form triple (three consecutive) Mg layers to sandwich the Gd-enriched quadruple layers. The ideal chemical formula of the structural block is $Mg_{35}Al_3Gd_4$ (Mg - 7.1 at.%Al - 9.5 at.%Gd). The crystal structure of the LPSO phase can thus be crystallographically described as one of the order-disorder (OD) structures, and the space group of either $P6_322$ or $R\bar{3}c$, is assigned when the simplest stacking of structural blocks is assumed.

Keywords: A. intermetallics, miscellaneous; B. crystallography; F. electron microscopy, transmission;

*Corresponding author: Kyosuke KISHIDA
Department of Materials Science and Engineering,
Kyoto University, Sakyo-ku, Kyoto 606-8501, JAPAN
E-mail address: kishida.kyosuke.6w@kyoto-u.ac.jp
Tel.: +81-75-753-5461; fax: +81-75-753-5461

1. Introduction

Because of the ever-increasing demands for light-weight structural materials, there is a great deal of attention to high-strength Mg alloys that can achieve high strength and high ductility simultaneously [1-3]. From this point of view, Mg alloys containing ternary Mg-TM (Transition-metal)-RE (Rare-earth) phases with long-period stacking-ordered (LPSO) structures have received a considerable amount of attention in recent years [4-9]. Although reasons why these alloys can simultaneously exhibit high strength and high ductility have been remained largely unsolved, ternary LPSO phases have been believed to play important roles in endowing them with excellent mechanical properties. When TM is Zn, LPSO phases in Mg-TM-RE ternary systems are reported to consist of structural blocks with five to eight close-packed atomic planes, forming various polytypes with different numbers of the close-packed atomic planes in the structural blocks and with different stackings of the structural blocks [10-19]. In the absence of the in-plane long-range ordering of the constituent atoms (as usually assumed in most studies in Mg-TM-RE LPSO phases), polytypes expressed as 10*H*, 14*H*, 18*R* and 24*R* polytypes (according to the Ramsdell notation) are reported to form, among which 14*H* and 18*R* polytypes are the most dominantly observed ones [10-19].

We have very recently investigated the crystal structure of a LPSO phase corresponding to the 18*R* polytype newly found to form in the Mg-Al-Gd system [17,18]. The crystal structure of the LPSO phase of the 18*R* type in the Mg-Al-Gd system is definitely different from those of LPSO phases in other Mg-TM-RE systems in that (1) the enrichment of RE (and TM) atoms occurs in four consecutive close-packed atomic planes in each structural block instead of two (this was confirmed to also be the case, at least, for the LPSO phase in the Mg-Zn-Y system in our previous study [17,18]) and that (2) long-range atomic ordering occurs in the four consecutive atomic planes in which the enrichment of RE (and TM) atoms occurs. Because of these characteristics, the LPSO phase in the Mg-Al-Gd system cannot be described as 'LPSO' phase any longer in a strict sense and the crystal structure is described with the concept of the order-disorder (OD) structure, in which a crystal structure is described with the symmetry of a structural block (an OD layer) and the relative relation between adjacent two OD layers [18,20-28]. With the layer group of $P(\bar{3})1m$ of the trigonal-type determined for the structural block (the OD layer), the OD-groupoid family for the 'LPSO' phase in the Mg-Al-Gd system is described using the so-called OD-groupoid symbols proposed by Dornberger-Schiff [18, 21, 22, 26-31], as follows.

$$\begin{matrix} P & 1 & 1 & 1 & \left(\bar{3}\right) & \frac{2}{m} & \frac{2}{m} & \frac{2}{m} \\ \left\{ \right. & 1 & 1 & 1 & \begin{pmatrix} \bar{3} \\ 3_3 \end{pmatrix} & \frac{2_{1/3}}{n_{1/3,2}} & \frac{2_{-1/3}}{n_{1/3,2}} & \frac{2}{n_{-2/3,2}} \left. \right\} \end{matrix} \quad (1).$$

The readers are referred to [21, 22, 26-31] for the meaning of the OD-groupoid symbols and some detailed discussion will also be made in the present paper. The expression for the crystal structure of the 'LPSO' phase corresponding to the 18*R* polytype in the Mg-Al-Gd system is thus quite different from those of LPSO phases in other Mg-TM-RE systems. This stems from the fact that the long-range atomic ordering occurs in the four consecutive atomic planes in which the enrichment of RE (and TM) atoms occurs. For LPSO phases of other types, however, nothing is known about the number of close-packed atomic layers in which the enrichment of RE (and TM) atoms occurs (usually assumed to be two in most previous studies) and whether or not long-range atomic ordering occurs in these RE (and TM)-enriched atomic layers. In view of the fact that the LPSO phases of the 14*H* polytype are observed as frequently as those of the 18*R* polytype are, it is of particular interest to determine the crystal structure of the LPSO phase of the 14*H* type as in the case of that of the

18*R* type found in the Mg-Al-Gd system.

In the present study, we investigate the crystal structure of a 'LPSO' phase in the Mg-Al-Gd system formed locally as 14*H* type in the same ingot used in our previous study to investigate the crystal structure of the 18*R*-type LPSO phase, by means of scanning transmission electron microscopy (STEM). We focus primarily on the detection of the in-plane ordering of Gd (and possibly Al) atoms in the close-packed atomic planes in which the enrichment of Gd and Al atoms are expected to occur and on the full description of the crystal structure with the concept of the OD theory. Then, we expand our analysis to the other LPSO phases composed of structural blocks with different numbers of layers, i.e. 10*H* (5-layers) and 24*R* (8-layers) in Mg-Al-Gd alloys in order to establish general ways to describe their crystal structures with the OD theory and to deduce simple polytypes based on the OD theory. Finally, we describe how to distinguish the OD-type LPSO phases with previously reported (disordered) LPSO phases by electron diffraction in transmission electron microscopy (TEM).

2. Experimental procedures

Ingots of a Mg-Al-Gd ternary alloys with a nominal composition of Mg - 3.5 at.%Al - 5.0 at.%Gd were produced by high- frequency induction-melting in an argon atmosphere. The ingots were homogenized at 550 °C for 2 hours and then heat-treated at 400 °C for 10 hours. Microstructures were examined by STEM with a JEM-2100F electron microscope operated both at 200 kV. Specimens for STEM observations were cut from heat-treated ingots, mechanically polished, and electropolished in a solution of perchloric acid (60 %), n-butyl alcohol and methanol (3:30:130 by volume) with 0.2 M of LiCl under 17 V at -55 °C.

3. Results

3.1. Stacking and in-plane atomic arrangements within each structural block

In the Mg-Al-Gd alloys, the LPSO phase with the 14*H*-type stacking sequence is rarely observed, unless it appears as a small part in an intergrowth structure with a few to a several structural blocks consisting of seven close-packed planes. While the 18*R*-type LPSO phase dominates in the intergrowth structure, the 14*H*-type LPSO phase often appear in the peripheries of the interface between the Mg matrix and 18*R*-type LPSO phases together with thin plates with 10*H*- and 24*R*-type stacking, as shown in the low-magnification high-angle annular dark-field (HAADF)-STEM image of Fig. 1. Atomic-resolution HAADF-STEM images of the 14*H*-type LPSO phase taken along $[2\bar{1}\bar{1}0]$[†] and $[1\bar{1}00]$ directions from the same region are shown in Figs. 2(a) and (b), respectively. Because of the strong contrast dependence on the average atomic number Z in the atomic columns in the HAADF-STEM image [17, 18, 32-35], atomic columns enriched with heavy Gd atoms are imaged as brighter spots in Figs. 2(a) and (b). It is apparent from the images that the Gd enrichment occurs in the four consecutive close-packed planes instead of two, which has been repeatedly reported for other Mg-TM-RE LPSO phases [15, 16]. The occurrence of the in-plane ordering of the Gd atoms in the four consecutive Gd-enriched planes is obvious, as will be described in detail later. If the in-plane ordering of the Gd atoms in the four consecutive Gd-enriched planes is ignored, the stacking sequence of the present 14*H*-type LPSO phase in the Mg-Al-Gd system

[†] Since the unit cell of the LPSO phase in the Mg-Al-Gd system cannot unambiguously be determined because of the stacking disorder of structural blocks along the direction perpendicular to the close-packed planes, Miller-Bravais indices and Weber symbols to express planes and directions for the LPSO phase, respectively, are referred to as those of the matrix phase of Mg with the h.c.p. structure unless otherwise stated.

is identical to that previously reported for the other Mg-TM-RE LPSO phases of the 14*H* type, as indicated in Fig. 2(a) [14-16]. Two types of structural blocks, each of which consists of seven close-packed atomic planes, with ABABCAC and ACACBAB stackings are identified to stack alternatively. The stacking sequence of these two-types of structural blocks are obviously related with each other in the twin relationship with the mirror plane being the central Mg layer in the stacking position A of the three consecutive Mg layers (Fig. 2(a)). These two types of the structural blocks are hereafter designated δ and δ_T blocks, respectively. If the twin relationship is taken into account, the atomic arrangements of these two-types of structural blocks are identical with each other. The present LPSO phase of the 14*H* type is thus confirmed to be formed by stacking these two types of seven close-packed layer structural blocks, which are related in the twin relation with each other.

The in-plane ordered arrangement of Gd and Al atoms in the four Gd-enriched layers with an f.c.c. type stacking sequence in the structural block is confirmed to be identical to that of 18*R*-type Mg-Al-Gd LPSO phase reported in our previous paper [18] through careful inspection of the arrangement of the brighter spots in the HAADF-STEM images. The in-plane long-range ordering in the four consecutive atomic planes can be described to occur so as to locate Al_6Gd_8 clusters with the $L1_2$ type atomic arrangement on lattice points of a $2\sqrt{3}a_{Mg} \times 2\sqrt{3}a_{Mg}$ primitive hexagonal lattice, where a_{Mg} is referred to the length of the unit vector along the *a*-axis of Mg [18]. Atomic arrangements in each of the seven atomic planes in the structural block together with the periodic arrangement of Al_6Gd_8 clusters in the quadruple layers projected along [0001] are depicted in Fig. 3 for the δ block with the stacking of the ABABCAC type. The inner two layers of the Gd-enriched quadruple layers are in B and C stacking positions with the chemical composition of $Mg_6Al_3Gd_3$, whereas the outer layers with the chemical composition of $Mg_{11}Gd$ are both in the A position. In addition, there exist three pure Mg layers in the structural block; two Mg layers in A and B positions and an Mg layer in the C position sandwich the Gd-enriched quadruple layers in the structural block. The ideal chemical formula of the structural block is calculated to be $Mg_{35}Al_3Gd_4$ (Mg - 7.1 at.%Al - 9.5 at.%Gd).

For the crystallographic description of the OD intermetallic phase, it is found to be suitable to assign the stacking sequences of the two structural blocks as (A)BABCAC(A)- and (A)CACBAB(A) for the δ and δ_T blocks, respectively, where the outer-most layers in the stacking position A common to the neighboring structural blocks are indicated with parenthesis so as to make easier to recognize both the symmetry of the structural block and symmetry relations between two adjacent blocks. The structural block is formed by assembling three-dimensional motif, whose point group is $\bar{3}m$ by setting the center of the Al_6Gd_8 cluster with the $L1_2$-type atomic arrangement as the center of the motif, on the two-dimensional primitive hexagonal lattice so that its three-fold rotoinversion axis is set perpendicular to the hexagonal lattice and its mirror planes become parallel to the lattice edges. The layer group of the structural block is then determined to be the trigonal-type of $P(\bar{3})1m$, as in the case of the 6-layer structural block of the 18R-type LPSO phase in the Mg-Al-Gd alloy [18]. The layer group is described with the Dornberger-Schiff notation, which is based on the Hermann-Mauguin symbols with additional parentheses indicating the direction of lacking periodicity [20, 36]. The details of the layer group symmetry will be described in the section 4.1.1.

3.2. Stacking of the structural blocks (Inter-structural block stacking)

In the present section, stacking relations between two neighboring structural blocks are examined by taking an example of the stacking of the δ_T-block on top of the δ-block. In the case of the stacking of the structural blocks of the 14*H*-type LPSO phase, the stacking

relations are described with a combination of translation and mirror reflection with respect to the plane perpendicular to the stacking direction. Considering the symmetry of the structural block (the layer group of $P(\bar{3})1m$), the mirror reflection is identical to 60°-, 180°-, and 300°-rotations about the axis passing perpendicularly the corner of the in-plane unit cell. Since the mirror reflection is common to all possible stacking relations, the difference in the stacking relations is characterized by the translation relations. As in the case of the 18*R*-type Mg-Al-Gd LPSO phase, the difference in the translation relations can be distinguished by examining the relative positions of the Gd atoms in the outer layers of the quadruple Gd-enriched layers for the two neighboring structural blocks, since two outer Gd-enriched layers in each structural block always take the same stacking position of A (Fig. 2) and the positions of the Gd atoms in these outer layers can be set so as to take only the corner positions of the in-plane $2\sqrt{3}a_{\mathrm{Mg}} \times 2\sqrt{3}a_{\mathrm{Mg}}$ unit cell (Figs. 3(c) and (f)). Since the in-plane unit of the structural block is 12-times larger than that of h.c.p. (hexagonal close-packed) Mg, there are 12 different translation relations between neighboring structural blocks. However, the layer group symmetry of $P(\bar{3})1m$ reduces these 12 translation relations into four, namely A_1, A_2, A_3 and A_4, which possess 1, 2, 3 and 6 crystallographically equivalent translation positions, respectively (Fig. 4). The propensity for these four translation relations can be determined through statistical analysis of the relative shifts of the positions of the Gd-enriched columns in the outer layers occurring among neighboring structural blocks in HAADF-STEM images. In HAADF-STEM images with the $<2\bar{1}\bar{1}0>$ incidence (Fig. 5(a)), the expected relative shift is 0 for the A_1 and A_2 positions and either 0 or 1/2 for the A_3 and A_4 positions, when measured in the unit of the distance between neighboring Gd-enriched columns in the outer layers. In HAADF-STEM images with the $<1\bar{1}00>$ incidence (Fig. 5(b)), on the other hand, the expected relative shift is 0 for the A_1 position, 1/3 for the A_2 position, either 0 or 1/2 for the A_3 position and either 1/6 or 1/3 for the A_4 positions in the unit of the distance between neighboring Gd-enriched columns in the outer layers. Since the observed shifts are dominantly 0 and 1/3 (more than 90%) respectively for the HAADF-STEM images with $<2\bar{1}\bar{1}0>$- and $<1\bar{1}00>$ incidences, the stacking relation of the type A_2 is found to be dominant in the 14*H*-type LPSO phase in the Mg-Al-Gd system. For the stacking relations of the type A_2, there exist two crystallographically equivalent translation relations described with the following vectors (Fig. 6),

$$\boldsymbol{t}_1 = \frac{2}{3}\boldsymbol{a}_1 + \frac{1}{3}\boldsymbol{a}_2 + \boldsymbol{c} \quad (2a)$$

$$\boldsymbol{t}_2 = \frac{1}{3}\boldsymbol{a}_1 + \frac{2}{3}\boldsymbol{a}_2 + \boldsymbol{c} \quad (2b),$$

where the vectors $\boldsymbol{a}_1$, $\boldsymbol{a}_2$ and $\boldsymbol{c}$ correspond to two in-plane unit vectors of the structural blocks and a unit vector of the 7-layer structural block along the stacking direction, respectively. Although the volume of the present 14*H*-type LPSO phase is too small (only in a thickness of a few to a several structural blocks) to check whether the stacking of structural blocks is fully-ordered or disordered, the existence of the two crystallographically equivalent translation relations ($\boldsymbol{t}_1$ and $\boldsymbol{t}_2$) indicates that the present 14*H*-type LPSO phase possesses the characteristics of the OD structure and is expected to exhibit stacking disorder of structural blocks similarly to the case of the 18*R*-type LPSO phase in the Mg-Al-Gd system [18].

4. Discussion

4.1. Structure description with the order-disorder (OD) theory

4.1.1. OD groupoid symbol

As described in the previous section, the 14*H*-type LPSO phase in the Mg-Al-Gd system is expected to exhibit one dimensional stacking disorder because of the existence of

two crystallographically equivalent stacking positions for the stacking of the fully-ordered structural blocks, as in the case of the 18*R*-type LPSO phase in the Mg-Al-Gd system. The crystal structure of the present LPSO phase can thus be described crystallographically with the concept of the order-disorder (OD) theory. In the OD theory, a crystal structure is described with partial symmetry operations (POs) transforming a structural block (an OD layer) into itself (λ-POs) and those transforming an OD layer into an adjacent one (σ-POs) [20-31].

Figure 7(a) shows atomic arrangement of the Al_6Gd_8 cluster characterizing the symmetry of the motif projected along the stacking direction and a corresponding symbolic figure for the motif. The symmetry of the point group of $\bar{3}m$ is schematically represented with the symbolic figure, in which *z*-coordinates of white and black triangles possess positive and negative values, respectively. The layer group symmetry of $P(\bar{3})1m$, which corresponds to λ-POs of the OD layer, can easily be recognized by examining symmetry relations among these triangles in the symbolic figures located on each lattice point of the hexagonal lattice as shown in Fig. 7(b). All graphical symbols representing symmetry operations refer to those defined in the international tables for crystallography [21, 26, 28, 29, 36, 37]. The symmetry operations of σ-POs correlating two neighboring OD layers can be determined through careful inspection of symmetry relations between two motifs on two neighboring OD layers. Figure 7(c) shows a schematic illustration of superposition of two OD layers (indexed as L_0 and L_1) correlated with the translation vector of $\boldsymbol{t}_1$ and the subsequent 60°-rotation about the axis passing perpendicularly the corner of the in-plane unit cell. In Fig. 7(c), the L_0 and L_1 layers are illustrated in black and gray colors, respectively. Figure 7(c) illustrates all σ-POs correlating the two motifs with respect to the seven specific directions; $\boldsymbol{a}_1$, $\boldsymbol{a}_2$, $\boldsymbol{a}_3$, $\boldsymbol{c}$, $\boldsymbol{a}_2 - \boldsymbol{a}_3$, $\boldsymbol{a}_3 - \boldsymbol{a}_1$ and $\boldsymbol{a}_1 - \boldsymbol{a}_2$ ($\boldsymbol{a}_1$, $\boldsymbol{a}_2$ and $\boldsymbol{a}_3$ correspond to the unit vectors of the OD layer with the two-dimensional hexagonal lattice, and $\boldsymbol{c}$ corresponds to the unit vector along the direction of missing periodicity, i.e. the stacking direction, the vector length of which is equal to the thickness of the structural block). For example, two motifs located on the lattice points correlated with the translation vector $\boldsymbol{t}_1$ in the figure are correlated with a combination of a counterclockwise rotation by 60° about the line 1/3, 2/3, *z* and a translation with the unit vector $\boldsymbol{c}$, a combination of a 180° rotation about the line 1/3, 1/6, *z* and a translation with the unit vector $\boldsymbol{c}$, and a clockwise rotoinversion by 60° about the line 1/3, 0, *z*, all of which are indicated with graphical symbols for 6_1, 2_1 and $\bar{6}$ in the figure, respectively. The determined POs for the present 14*H*-type LPSO phase in the Mg-Al-Gd system can be described with the so-called OD-groupoid symbol as follows,

$$\begin{matrix} P & 1 & 1 & 1 & \left(\bar{3}\right) & \frac{2}{m} & \frac{2}{m} & \frac{2}{m} \\ \left\{ \begin{matrix} \frac{2_1}{n_{1/3,2}} & \frac{2}{n_{-2/3,2}} & \frac{2_{-1}}{n_{1/3,2}} & \begin{pmatrix} \bar{6} \\ 2_2 \\ 6_6 \\ n_{1,1/3} \end{pmatrix} & 1 & 1 & 1 \end{matrix} \right\} \end{matrix} \quad (3),$$

Here, the first line represents the symmetry of the layer group of $P(\bar{3})1m$ and the second line represents the symmetry operations correlating two adjacent OD layers, both of which are indicated with respect to the seven specific directions; $\boldsymbol{a}_1$, $\boldsymbol{a}_2$, $\boldsymbol{a}_3$, $\boldsymbol{c}$, $\boldsymbol{a}_2 - \boldsymbol{a}_3$, $\boldsymbol{a}_3 - \boldsymbol{a}_1$ and $\boldsymbol{a}_1 - \boldsymbol{a}_2$. The notations used for σ-POs in the second line of eq. (3) are similar to those defined in the international tables for crystallography A [20, 21, 24-31, 37]. For example, the symbol of 6_6 in the fourth position of the second line indicates a sixfold screw axis parallel to the $\boldsymbol{c}$ axis with a translation of $\boldsymbol{c}$, and the symbol of $2_1/n_{1/3,2}$ in the first position of the second line represents a twofold screw axis parallel to the $\boldsymbol{a}_1$ axis with a translation of $\boldsymbol{a}_1/2$ and a *n*-glide

normal to the $\boldsymbol{a}_1$ axis with translational component of $(\boldsymbol{a}_2\text{-}\boldsymbol{a}_3)/6 + \boldsymbol{c}$, which are indicated with two numbers in subscripts corresponding to twice of translation components with respect to two specific unit vectors, namely $(\boldsymbol{a}_2\text{-}\boldsymbol{a}_3)$ and $\boldsymbol{c}$, respectively. Although the layer group for the structural block of the 14*H*-type LPSO phase in the Mg-Al-Gd system is identical to that of the 18*R* type, the σ-POs correlating two adjacent OD layer are completely different due mainly to the existence of the 60°-rotation relation about the axis passing perpendicularly the corner of the in-plane unit cell.

4.1.2. Polytypes with the maximum degree of order (MDO polytypes)

In the OD theory, the number of crystallographically equivalent translation relations (equivalent stacking positions) between two neighboring structural blocks (OD layers) can be evaluated by the so-called NFZ relation [22, 28, 30, 31]. The numbers N and F are defined as the general multiplicity of the group of the POs that do not change the sign of z-coordinate among λ-POs (denoted as λ-τ-POs) and as that of the subgroup of the λ-τ-POs which are commonly valid for neighboring OD layers, respectively. The number of Z, which corresponds to the number of the possible distinct stacking positions of an OD layer L_{p+1} located on top of the fixed position of a neighboring layer L_p (p: integer), can be obtained as a function of N and F. In the case of the 14*H*-type LPSO phase in the Mg-Al-Gd system, $N = 6$ and $F = 3$ (only three symmetry operations, identity (1), a counter clockwise rotation by 120° around the line 0, 0, z (3^+) and a clockwise rotation by 120° around the line 0, 0, z (3^-), are common to the two neighboring OD layers). The formulae for estimating the number of Z depend also on the category of the OD structure [28, 30]. Since the OD groupoid family described with eq. (3) is confirmed to be categorized as the category Ia according to the available POs, the number of Z is finally calculated to be $Z = N/F = 2$. The number of the equivalent stacking positions, i.e. the translation relations for the present OD groupoid family is crystallographically confirmed to be 2, which is consistent with what was described in the section 3.2. The numbers of F and Z as well as the OD groupoid symbols similarly deduced for all possible stacking positions A_1 to A_4 are summarized in Table 1. Since the number of Z for the stacking position A_1 is equal to 1, the crystal structure derived by this stacking type should not be described as an OD structure but as a fully ordered structure, the space group of which is determined to be $P6_3/mcm$.

We now derive some simple polytypes designated as those with maximum degree of order (MDO polytypes) for the OD groupoid family described with eq. (3) [21, 22, 27-31, 38-42]. The MDO polytypes are defined as polytypes in which not only pairs, but triples, quadruples etc. of consecutive OD layers are geometrically equivalent [28-31, 38-42]. Each MDO polytype is derived by continuous application of a generating operation. Characteristics of such a generating operation are that (1) the operation possesses a translational component along the stacking direction and (2) the operation correlating L_0 with L_1 is commonly valid to correlate any pairs of L_p and L_{p+1} (p: integer). Among all σ-POs for the OD groupoid family, 6_6, 2_2 and n-glide normal to the $\boldsymbol{a}_i$ axes (i = 1,2,3) are considered to be possible candidates from the characteristic (1). If each of these operations is commonly valid for any neighboring OD layer pairs (the characteristic (2)), then the operation is considered as a generating operation. One of such generating operations among all σ-POs for the OD groupoid family is 6_6, as shown in Fig. 7(b) and eq. (3). A continuous application of this generating operation of 6_6 (a counter-clockwise rotation by 60° about the line 1/3, 2/3, z and a translation with the unit vector $\boldsymbol{c}$) yields a MDO polytype with a hexagonal cell, whose c-axis is six-times longer than that of the thickness of the structural block. However, with the sixfold symmetry of the structural block, the minimum repeat distance along the stacking direction $\boldsymbol{c}$ can be reduced to twice that of the thickness of the structural block. Thus, the MDO polytype derived by the generating operation of 6_6 is found to possess a hexagonal cell ($\boldsymbol{a}_{H1} = \boldsymbol{a}_1$, $\boldsymbol{a}_{H2} = \boldsymbol{a}_2$ and $\boldsymbol{c}_H = 2\boldsymbol{c}$,

where $\boldsymbol{a}_{H1}$, $\boldsymbol{a}_{H2}$ and $\boldsymbol{c}_H$ are unit vectors for the hexagonal cell), in which the generating operation of 6_6 becomes a total operation of 6_3. This MDO polytype is composed of two structural blocks of δ and δ_T (14 close-packed layers), and therefore is assigned to be 2*H* in the Ramsdell notation. In this MDO polytype, the σ-POs of 2_2 are commonly valid and become twofold screw operations in the three-dimensional hexagonal cell. In addition, the σ-POs of 2 parallel to the secondary directions ($\boldsymbol{a}_i$, i = 1,2,3) become two-fold rotation operations around the secondary axes in the three-dimensional hexagonal unit cell. The λ-POs of 2 around the tertiary directions ($\boldsymbol{a}_i - \boldsymbol{a}_j$,, i, j = 1,2,3, $i \neq j$) in each OD layer become two-fold rotation operations around lines parallel to the tertiary axes at z = 1/4, 3/4 etc. in the three-dimensional hexagonal unit cell. The space group for this MDO polytype is thus assigned to be of $P6_322$. The same MDO polytype is confirmed to be derived by a continuous application of a generating operation of 2_2 about the line 1/3, 1/6, z. Another generating operation is the glide operation of $n_{-2/3,2}$ with respect to the plane perpendicular to the $\boldsymbol{a}_2$ axis of the structural block, whose continuous application derives another MDO polytype with a rhombohedral cell ($\boldsymbol{a}_{R1} = \boldsymbol{a}_1$, $\boldsymbol{a}_{R2} = \boldsymbol{a}_2$ and $\boldsymbol{c}_R = 6\boldsymbol{c}$, where $\boldsymbol{a}_{R1}$, $\boldsymbol{a}_{R2}$ and $\boldsymbol{c}_R$ are unit vectors for the rhombohedral cell). This second MDO polytype is formed with six OD layers, and therefore is assigned to be 6*R* in the Ramsdell notation. For this MDO polytype, the glide operation of $n_{-2/3,2}$ and the two-fold rotation operations around lines parallel to the $\boldsymbol{a}_2$ axis among the σ-POs expressed in eq. (3) are confirmed to become a *c*-glide operation and total two-fold rotation operations valid for the whole rhombohedral cell, respectively. In addition, a three-fold rotoinversion operation in the λ-POs becomes a total operation of the same type for the whole rhombohedral cell. Consequently, the whole structure of the second MDO polytype is found to possess a space group symmetry of $R\bar{3}c$. Crystallographic information such as space groups, the Ramsdell notations and lattice constants for these MDO polytypes is summarized in Table 1. Some MDO polytypes belonging to other OD groupoid families characterized by the stacking positions A_3 and A_4 are deduced in the similar way and their crystallographic information is also summarized in table 1.

4.1.3. Prediction of crystal structures for LPSO phases with 10H- and 24R-type stacking sequences

Since different polytypes expressed as 10*H*, 18*R*, 14*H* and 24*R* types consisting respectively of 5, 6, 7 and 8 close-packed atomic planes are reported to form as LPSO phases in Mg-TM-RE alloy systems [10-19], it may be helpful to describe their possible crystal structures with the concept of the OD theory. Indeed, thin plates corresponding to 10*H*- and 24*R*-type LPSO phases are observed occasionally as small parts of the intergrowth structure in the present Mg-Al-Gd system (Fig. 1). Atomic-resolution HAADF-STEM images of such small areas corresponding to 10*H*- and 24*R*-type LPSO phases are shown respectively in Figs. 8(a) and (b) with the $[2\bar{1}\bar{1}0]$ incident. It is evident that the enrichment of Gd atoms occurs in four consecutive atomic layers identically in the 5-layer and 8- structural blocks and that the in-plane atomic ordering in the quadruple Gd-enriched layers observed in these two cases (10*H*- and 24*R*-type LPSO phases) is exactly the same as that observed for 14*H*- and 18*R*-type LPSO phases with 6- and 7-layer structural blocks in the Mg-Al-Gd system. The fact that the atomic arrangement in the Gd-enriched quadruple layers is identical for all structural blocks whatever the number of close-packed layers (either 5, 6, 7 or 8) indicates that these structural blocks differ from each other only in the number pure-Mg layers with the h.c.p type stacking sequence and that all structural blocks possess the same layer group symmetry of $P(\bar{3})1m$. The stacking relations of these structural blocks can be classified into two types depending on the number of close-packed planes constituting the structural block. If the number of the close-packed planes is odd, the stacking relations can be described in a way exactly the same as that used for the 14*H*-type LPSO phase with 7-layer structural

blocks, as described in the present paper. In this case, the possible stacking positions, OD-groupoid symbols and space groups for MDO polytypes are common to those summarized in Table 1. On the other hand, if the structural block is composed of an even number of the close-packed layers, the stacking relations can be described in a way exactly the same as that used for the 18*R*-type LPSO phase with 6-layer structural blocks, as described in our previous paper [18]. Table 2 summarizes OD groupoid symbols and crystallographic information of some MDO polytypes for three OD groupoid families generated by three stacking types (C_1, C_2 and C_3) for the LPSO phase composed of the 6-layer structural blocks described in our previous paper [18].

4.2. Identification of the OD character with electron diffraction patterns

The OD character of Mg-TM-RE LPSO phases can easily be identified by inspecting their electron diffraction patterns. If the LPSO phase is a member of an OD groupoid family, there should be two different kinds of reflections, so-called 'OD family reflections' that are common to all possible polytypes in the family and 'characteristic reflections' that appear at different positions in the electron diffraction pattern depending on polytype. The latter reflections sometimes appear as sharp steaks elongated along the stacking direction if some different OD polytypes are incorporated [18, 29, 30].

We now discuss how the OD character of Mg-TM-RE LPSO phases can be identified from electron diffraction patterns by taking an example of the 14*H*-type Mg-Al-Gd LPSO phase whose OD groupoid family is described by eq. (3). The reflection conditions of the OD family reflections for the present 14*H*-type LPSO phase can be obtained by considering those for a fictitious superposed structure (termed as a family structure), which is obtained by simultaneously applying two possible stacking relations described in the section 3.2. The family structure is confirmed to have a $2a_{\mathrm{Mg}} \times 2a_{\mathrm{Mg}} \times 2h$ hexagonal unit cell with a space group of $P6_3/mmc$, where h corresponds the height of the 7-layer structural block. Approximate crystallographic information is described in appendix. Then, the reflection conditions for the OD family reflections are expressed as follows.

$$\begin{aligned} &H\,H\,\overline{2H}\,L\!:\!L = 2n \ \ (n:\text{integer}) \\ &0\,0\,0\,L\!:\!L = 2n \ \ (n:\text{integer}) \end{aligned} \qquad (4),$$

where the indices with capital letters are referred to the unit cell of the OD family structure. The calculated selected-area electron diffraction (SAED) patterns based on the reflection conditions (eq. (4)) with the $[2\bar{1}\bar{1}0]_{\mathrm{F}}$ and $[1\bar{1}00]_{\mathrm{F}}$ incidences of the OD family structure (the subscript 'F' refers to the family structure), which correspond respectively to $[2\bar{1}\bar{1}0]$ and $[1\bar{1}00]$ incidences of the h.c.p. structure, are illustrated in Figs. 9(a) and (e), together with those calculated for the 2*H* MDO polytype (Figs. 9(b) and (f)) and for the 6*R* MDO polytype (Figs. 9(c) and (g)). The SAED patterns calculated with the same incidences for a 14*H*-type LPSO phase without atomic ordering of Gd and Al (hereafter designated as a disordered LPSO phase) are shown also in Figs. 9(d) and (h) for references. The calculation of SAED patterns was carried out with the use of the NCEM's image simulation software package NCEMSS [42]. For the two MDO polytypes, the OD family reflections indeed appear commonly in the reciprocal lattice rows indicated with white arrows in the figures. Other reflections in the reciprocal lattice rows marked with black arrows in the figures are not common to the two MDO polytypes (2*H* and 6*R*) and they appear in different positions in these reciprocal lattice rows depending on polytype. These reflections are characteristic reflections that are specific for each of the MDO polytypes in the OD family described by eq. (3). Therefore, if the 14*H*-type LPSO phase exhibits the OD character in which one dimensional disorder occurs for the stacking of structural blocks, the characteristic reflections should appear as sharp streaks extending along the stacking direction in their corresponding

reciprocal lattice rows, while the family reflections appear as sharp and discrete diffraction spots in their corresponding reciprocal lattice rows.

Comparison of the SAED patterns for the family structure (Figs. 9(a) and (e)) and the MDO structures (Figs. 9(b), (c), (f) and (g)) with those for the disordered LPSO phase (Figs. 9(d) and (h)) reveals that the OD structure described by eq. (3) generates the OD family reflections in the $n/2[01\bar{1}l]^*$ and $n/2[11\bar{2}l]^*$ reciprocal lattice rows (n: odd integer) in the SAED patterns of the $[2\bar{1}\bar{1}0]$ and $[1\bar{1}00]$ incidences, respectively, together with the characteristic reflections in the $n/6[11\bar{2}l]^*$ reciprocal lattice rows ($n = 6m+1$, $6m+2$, $6m+4$ and $6m+5$, m = integer). The reciprocal lattice rows for both the OD family reflections and the characteristic reflections are identical for 14*H*- and 18*R*-type LPSO phases with the OD structures described by the eq. (3) and eq. (1), respectively [18]. Inclusion of other types of block stacking corresponding to other OD structure causes some complexity in the SAED pattern by adding streaks also in the $n/2[01\bar{1}l]^*$ and $n/2[11\bar{2}l]^*$ reciprocal lattice rows (n: odd integer) of the OD family reflections, since an OD family structure and therefore the reflection conditions for the OD family reflections depends on the OD groupoid family. However, additional streaks should be very weak in intensity, since there should be a strong preference in the stacking positions if the LPSO phase tends to possess an OD structure. Thus, identification whether or not a particular LPSO phase possesses the OD character originating from the same type of atomic ordering of Gd and Al in the four consecutive close-packed planes and the same type of stacking preference can easily be made by inspecting the existence of both the sharp and discrete diffraction spots for the family reflections in the $n/2[01\bar{1}l]^*$ and $n/2[11\bar{2}l]^*$ reciprocal lattice rows (n = odd integer) and the sharp streaks for the characteristic reflections in the $n/6[11\bar{2}l]^*$ reciprocal lattice rows ($n = 6m+1$, $6m+2$, $6m+4$ and $6m+5$, m = integer).

5. Conclusion

The crystal structure of a 14*H*-type LPSO phase formed in a Mg-Al-Gd alloy as a local small part in the intergrowth structure together with that of the 18*R*-type LPSO phase was investigated by s scanning transmission electron microscopy (STEM) and transmission electron microscopy (TEM). The results obtained are summarized as follows.

(1) The 14*H*-type LPSO phase in the Mg-Al Gd system is formed by stacking structural blocks, each of which is composed of seven close-packed atomic planes. In each structural block, Gd atoms are enriched in four consecutive atomic planes with an fcc-type stacking sequence. Gd and Al atoms are ordered in a long range within the four consecutive atomic planes, resulting in the periodic formation of Al_6Gd_8 clusters with the $L1_2$-type atomic arrangement. The symmetry of the structural blocks is expressed with the layer group of $P(\bar{3})1m$.

(2) There exist two crystallographically equivalent stacking relations for the preferential stacking of seven-layer structural blocks, which leads to the occurrence of one-dimensional stacking disorder for the 14*H*-type LPSO phase in the Mg-Al-Gd system.

(3) The structure of the 14*H*-type LPSO phase can be crystallographically described as one of the OD structures as expressed with the OD-groupoid symbols as follows,

$$P \quad 1 \quad 1 \quad 1 \quad \left(\bar{3}\right) \quad \frac{2}{m} \quad \frac{2}{m} \quad \frac{2}{m}$$

$$\left\{ \begin{array}{cccc} & & & \left(\begin{array}{c} \bar{6} \\ 2_2 \\ 6_6 \\ n_{1,1/3} \end{array} \right) \\ \dfrac{2_1}{n_{1/3,2}} & \dfrac{2}{n_{-2/3,2}} & \dfrac{2_{-1}}{n_{1/3,2}} & \end{array} \right. \quad 1 \quad 1 \quad 1 \quad \left. \right\}$$

(4) The space groups for the two simplest polytypes designated as 2*H* and 6*R* polytypes in the Ramsdell notation are determined to be $P6_322$ (#182: hexagonal) and $R\bar{3}c$ (#167: rhombohedral), respectively.

Acknowledgements

This work was supported by Grant-in-Aid for Scientific Research from the Ministry of Education, Culture, Sports, Science and Technology (MEXT), Japan. (No. 22656156, No. 23360306, and No. 23109002), in part by the Global COE (Center of Excellence) Program of International Center for Integrated Research and Advanced Education in Materials Science from the MEXT, Japan and in part by the Kumamoto Prefecture CREATE project from JST.

Appendix

Approximate crystallographic parameters for the family structure of the OD-groupoid family described by eq. (3). Space group: $P6_3/mmc$ (#194), $a = b = 2a_{Mg}$, $c = 2h$ (h corresponds to the height of the 7-layer structural block).

Atom	Site	*x*	*y*	*z*
Al(1)	12*k*	0.30	0.15	0.03
Gd(1)	4*e*	0	0	0.10
Gd(2)	12*k*	0.30	0.60	0.03
Mg(1)	2*b*	0	0	1/4
Mg(2)	4*f*	1/3	2/3	0.17
Mg(3)	6*h*	0.50	0.50	1/4
Mg(4)	12*k*	0.50	0.50	0.10
Mg(5)	12*k*	1/3	1/6	0.17

References

1. F.H. Froes, D. Eliezer and E. Aghion, JOM 50 (1998) 30-34.
2. A.A. Luo, Int. Mater. Rev. 49 (2004) 13-30.
3. M. Bamberger and G. Dehm, Annu. Rev. Mater. Res. 38 (2008) 505-533.
4. Y. Kawamura, K. Hayashi, A. Inoue and T. Masumoto, Mater. Trans. 42 (2001) 1172-1176.
5. A. Inoue, Y. Kawamura, M. Matsushita, K. Hayashi and J. Koike, J. Mater. Res. 16 (2001) 1894-1900.
6. Y. Kawamura, T. Kasahara, S. Izumi and M. Yamasaki, Scripta Mater. 55 (2006) 453-456.
7. Y. Kawamura and M. Yamasaki, Mater. Trans. 48 (2007) 2986-2992.
8. K. Hagihara, N. Yokotani and Y. Umakoshi, Intermetallics 18 (2010) 267-276.
9. K. Hagihara, A. Kinoshita, Y. Sugino, M. Yamasaki, Y. Kawamura, H.Y. Yasuda and Y. Umakoshi, Acta Mater. 58 (2010) 6282-6293.
10. Z.P. Luo and S.Q. Zhang, J. Mater. Sci. Lett. 19 (2000) 813-815.
11. E. Abe, Y. Kawamura, K. Hayashi and A. Inoue, Acta Mater. 50 (2002) 3845-3857.
12. D.H. Ping, K. Hono, Y. Kawamura and A. Inoue, Phil. Mag. Lett. 82 (2002) 543-551.
13. T. Itoi, T. Seimiya, Y. Kawamura and M. Hirohashi, Scripta Mater. 51 (2004) 107-111.
14. M. Matsuda, S. Ii, Y. Kawamura, Y. Ikuhara and M. Nishida, Mater. Sci. Eng. A393 (2005) 269-274.
15. M. Yamasaki, M. Saaki, M. Nishijima and K. Hiraga, Acta Mater. 55 (2007) 6798-6805.

16. Y.M. Zhu, A.J. Morton and J.F. Nie, Acta Mater. 58 (2010) 2936-2947.
17. H. Yokobayashi, K. Kishida, H. Inui, M. Yamasaki and Y. Kawamura, Mater. Res. Soc. Symp. Proc., 1295 (2011) 267-272.
18. H. Yokobayashi, K. Kishida, H. Inui, M. Yamasaki and Y. Kawamura, Acta Mater. 59 (2011) 7287-7299.
19. E. Abe, A. Ono, T. Itoi, M. Yamasaki and Y. Kawamura, Phil. Mag. Lett. 91, (2011) 690-696.
20. K. Dornberger-Schiff, Acta Cryst. 9 (1956) 593-601.
21. K. Dornberger-Schiff and H. Grell-Niemann, Acta Cryst. 14 (1961) 167-177.
22. K. Dornberger-Schiff, Abh. Dtsch. Akad. Wiss. Berlin, Kl. Chem. Geol. Biol. 3 (1964) p.1.
23. K. Dornberger-Schiff and K. Fichtner, Krist. Tech. 7 (1972) 1035-1056.
24. K. Fichtner, Krist. Tech. 12 (1977) 1263-1267.
25. K. Dornberger-Schiff, Krist. Tech. 14 (1979) 1027-1045.
26. K. Fichtner, Krist. Tech. 14 (1979) 1073-1078.
27. K. Fichtner, Krist. Tech. 14 (1979) 1453-1461.
28. S. Ďurovič, Fundamentals of the OD theory, in: S. Merlino (Ed.), Modular aspects of minerals / EMU Notes in Mineralogy, Vol. 1, Eötvös University Press, Budapest, 1999, pp. 3-28.
29. S. Merlino, OD approach in minerals: examples and applications, in: S. Merlino (Ed.), Modular aspects of minerals / EMU Notes in Mineralogy, Vol. 1, Eötvös University Press, Budapest, 1999, pp. 29-54.
30. G. Ferraris, E. Makovicky and S. Merlino, Crystallography of Modular Materials, Oxford University Press, New York, 2004.
31. S. Ďurovič, Layer stacking in general polytypic structures. Sect. 9.2.2, in: A.C.J. Wilson, E. Prince (Eds.), International Table for Crystallography, Vol. C, third ed., Springer, Dordrecht, 2004, pp. 760-773.
32. S.J. Pennycook and L.A. Boatner, Nature 336 (1988) 565-567.
33. S.J. Pennycook, M. Varela, C.J.D. Hetherington and A.I. Kirkland, MRS Bull. 31 (2006) 36-43.
34. S.J. Pennycook, A.R. Lupini, M. Varela, A.Y. Borisevich, Y. Peng, M.P. Oxley and M.F. Chisholm, *Scanning Transmission Electron Microscopy for Nanostructure Characterization. Chapter 6*, in: W. Zhou, Z.L. Wang (Eds.), Scanning Microscopy for Nanotechnology: Techniques and Applications, Springer, New York, 2006, pp. 152-191.
35. K. Kishida and N.D. Browning, Physica C 351 (2001) 281-294.
36. V. Kopský and D.B. Litvin DB (Eds.), International Table for Crystallography, Vol. E, second ed., John Wiley & Sons, Ltd., West Sussex, 2010.
37. Th. Hahn (ed.), International Table for Crystallography, Vol. A, fifth ed., Springer, Dordrecht, 2005.
38. K. Dornberger-Schiff, Acta Cryst. A38 (1982) 483-491.
39. K. Dornberger-Schiff, Acta Cryst. A38 (1982) 491-498.
40. S. Merlino and S. Zanardi, Atti. Soc. Tosc. Sci. nat. Mem. Serie A 111 (2006) 31-44.
41. J. Hybler and S. Ďurovič, Acta Cryst. A65 (2009) 501-511.
42. R. Kilaas, *Interactive simulation of high resolution electron micrographs*, in: G.W. Bailey (Ed.), Proc 45th Ann Meeting EMSA, San Francisco Press, San Francisco, 1987, pp. 66-69.

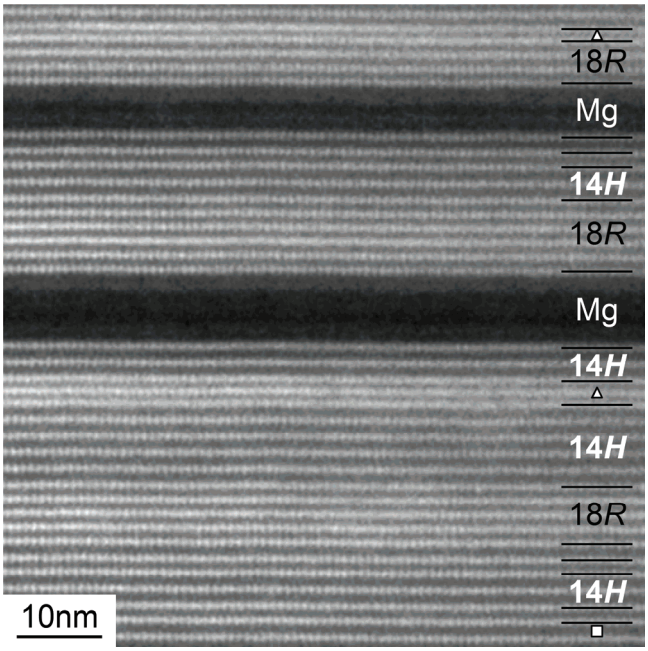

Fig. 1. A HAADF-STEM image of an intergrowth structure in a heat-treated Mg - 3.5 at.% Al - 5 at.% Gd alloy. Incident beam direction is parallel to $[1\bar{1}00]$. Triangles and a square indicate structural blocks corresponding to the 10*H*-type (five atomic layers) and 24*R*-type (eight atomic layers) LPSO phase, respectively.

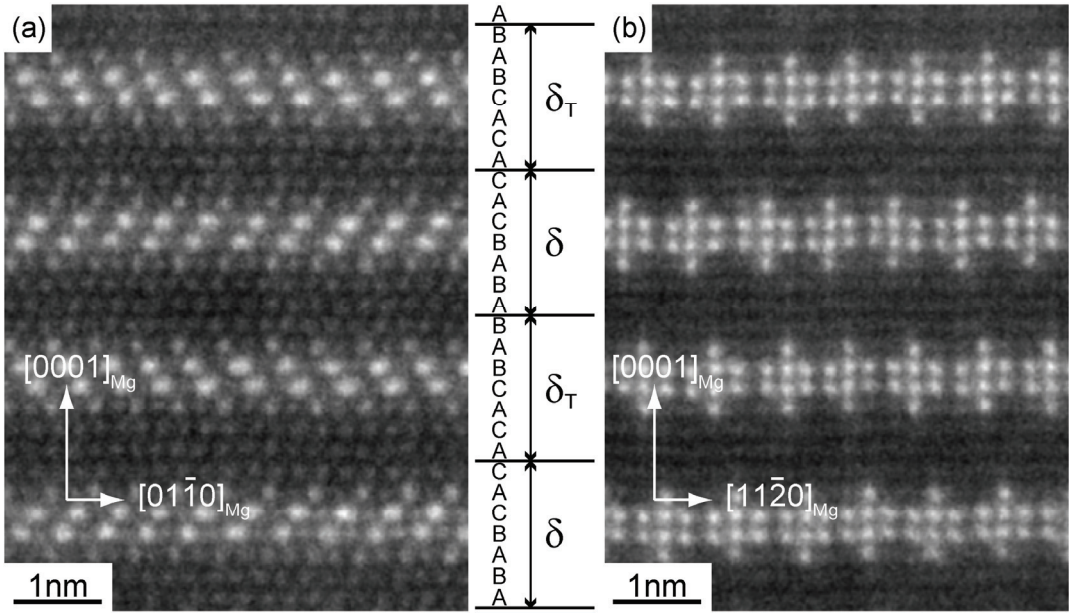

Fig. 2. Atomic resolution HAADF-STEM images of the 14*H*-type Mg-Al-Gd LPSO phase taken along (a) $[2\bar{1}\bar{1}0]$ and (b) $[1\bar{1}00]$.]

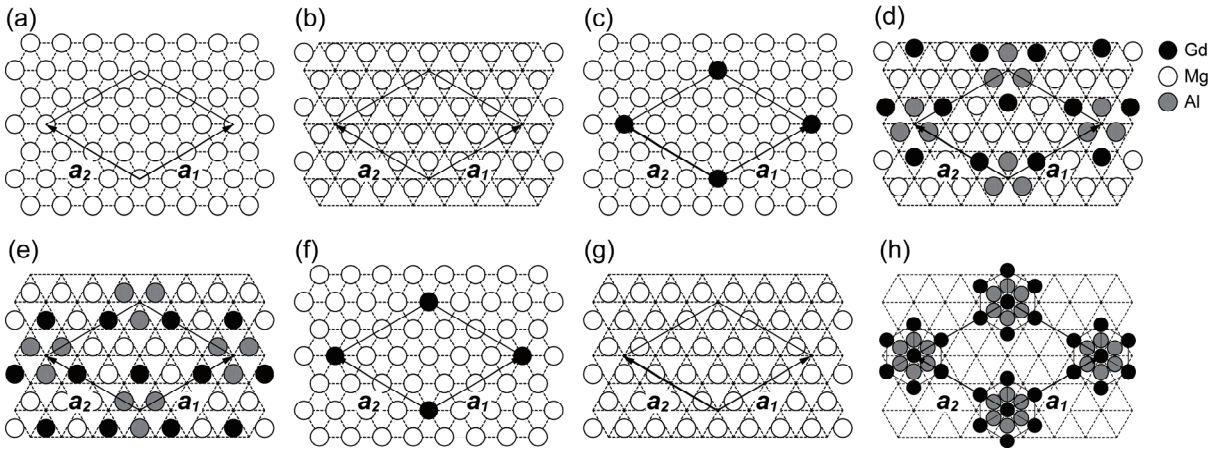

Fig. 3. (a-g) Atomic arrangements in each of the seven layers in the structural block with the stacking of ABABCAC (δ block) and (h) periodic arrangement of Al_6Gd_8 clusters in the quadruple layers projected along [0001]. (a), (b) and (g) are Mg layers in A, B and C stacking positions, (c) and (f) are the outer layers ($Mg_{11}Gd$) both in the A position, and (d) and (e) are the inner layers ($Mg_6Al_3Gd_3$) in B and C positions.

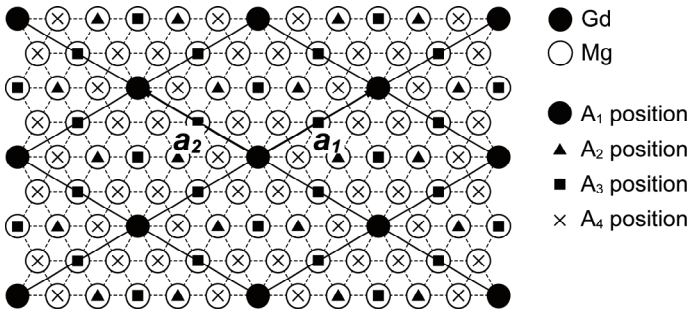

Fig. 4. Possible stacking positions of the δ_T block stacked on the δ block. Positions of δ_T blocks are indicated with those of the Gd atoms in the outer layers in the A positions.

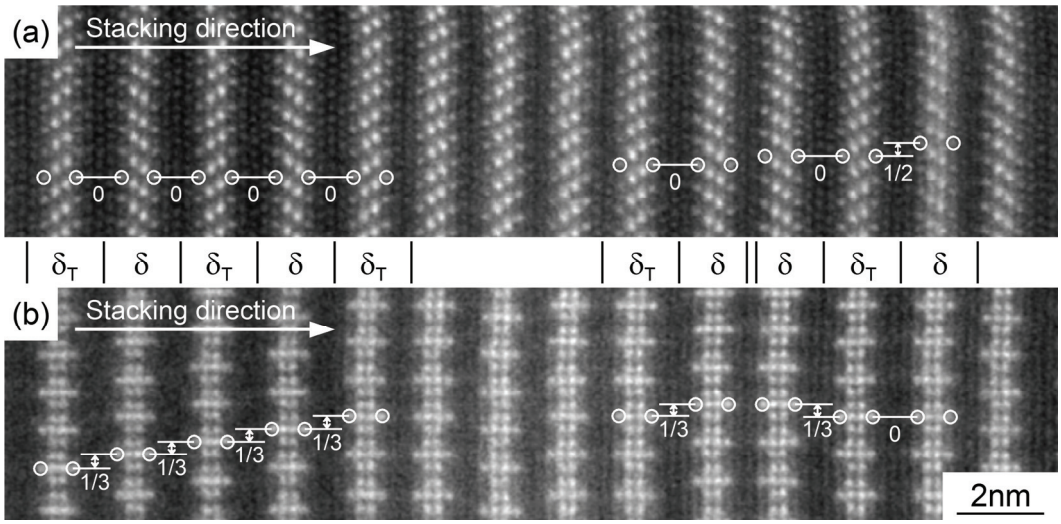

Fig. 5. Variation of the stacking sequence of the 7-layer structural blocks viewed along (a) $[2\bar{1}\bar{1}0]$ and (b) $[1\bar{1}00]$. The relative shifts of the stacking position for the Gd atoms in the outer layers occurring between neighboring structural blocks are indicated in the unit of the distance between neighboring Gd-enriched columns in the outer layers.

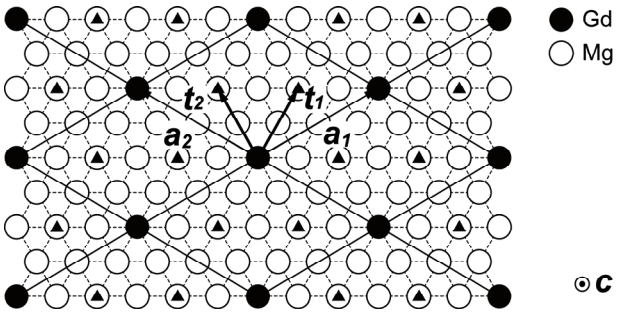

Fig. 6. Two crystallographically equivalent translation vectors $\boldsymbol{t}_1$ and $\boldsymbol{t}_2$ corresponding to the preferential stacking relations of the type A_2.

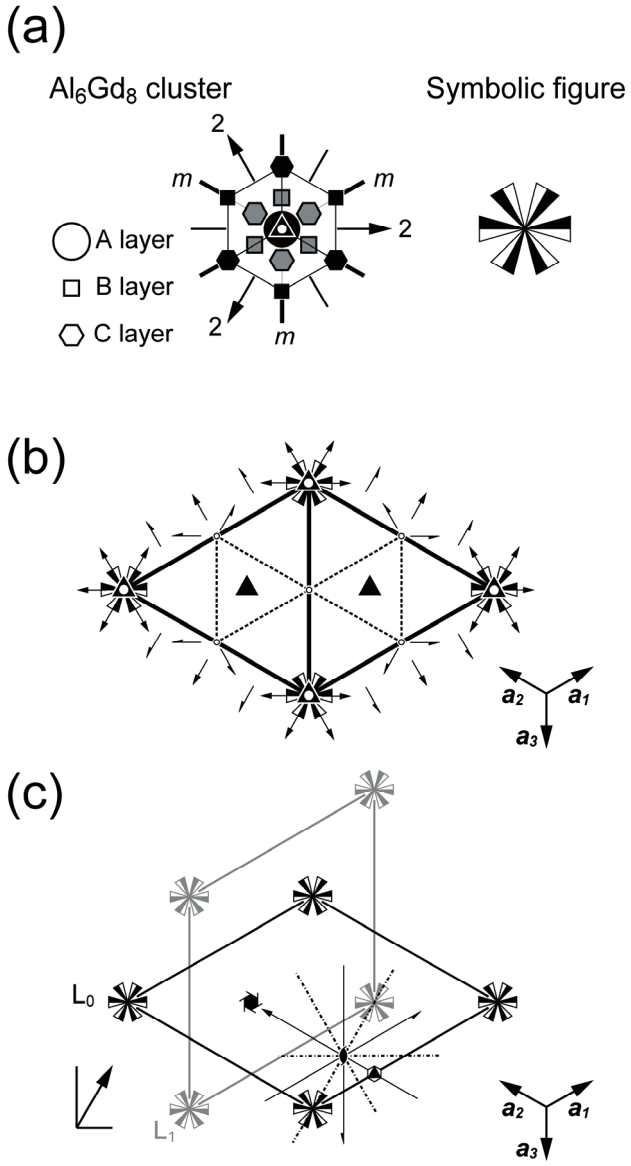

Fig. 7. (a) atomic arrangement of the Al_6Gd_8 cluster characterizing the symmetry of the motif projected along the stacking direction and a corresponding symbolic figure for the motif, (b) diagram of symmetry elements for the layer group of $P(\bar{3})1m$ corresponding to the λ-POs in the OD layer for the Mg-Al-Gd LPSO phase and (c) schematic illustration of the σ-POs transforming an OD layer (L_0) into an adjacent one (L_1).

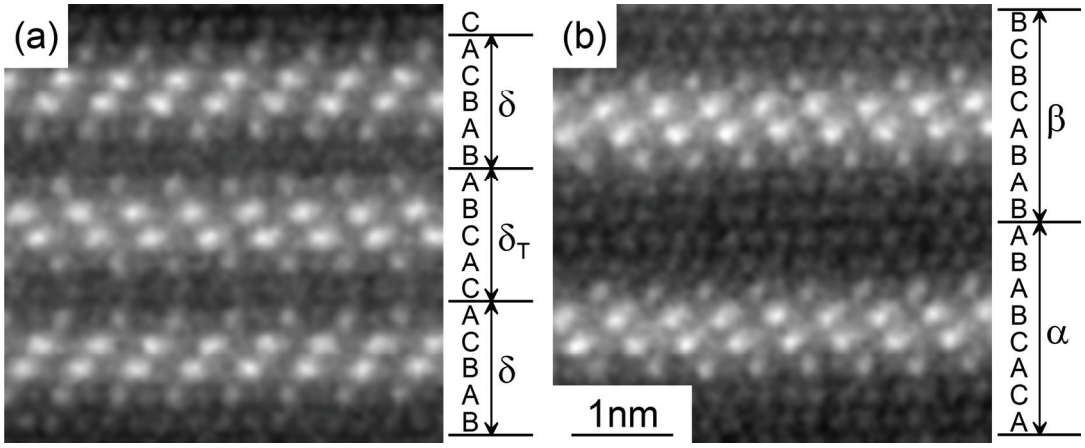

Fig. 8. Atomic resolution HAADF-STEM images of Mg-Al-Gd LPSO phases of (a) 10*H* and (b) 18*R* types taken along [$2\bar{1}\bar{1}0$].

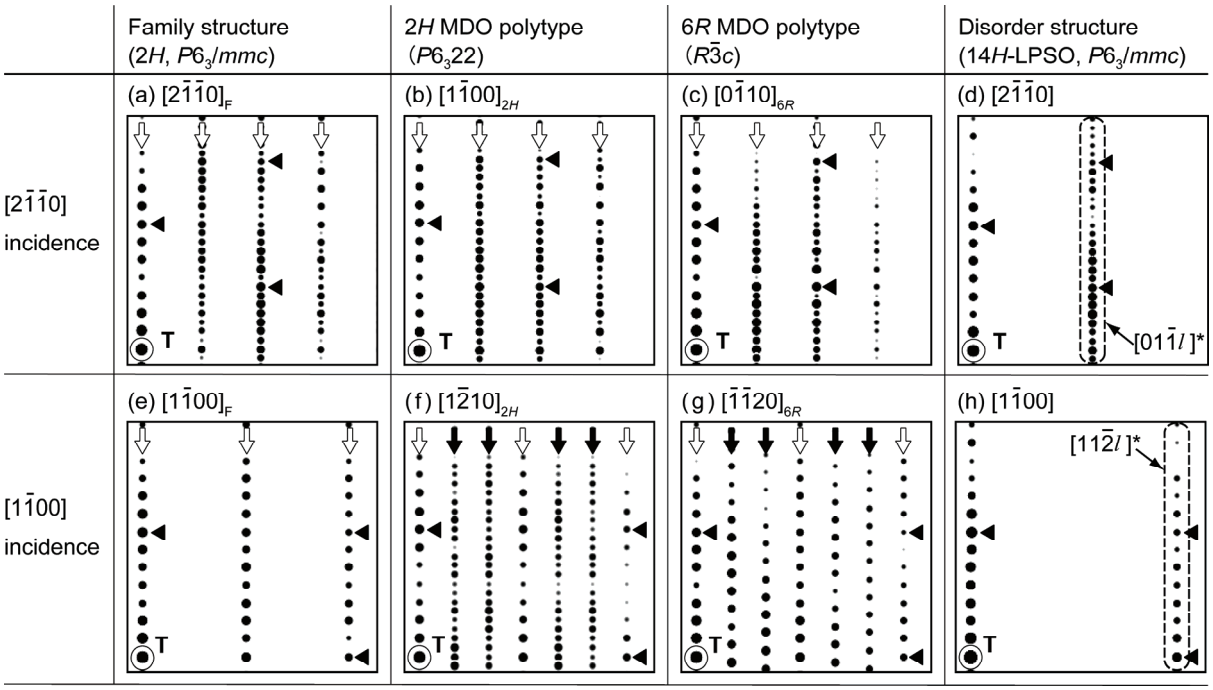

Fig. 9. SAED patterns in the [$2\bar{1}\bar{1}0$] and [$1\bar{1}00$] projections calculated for (a,e) the OD family structure, (b,f) the 2*H* MDO polytype, (c,g) the 6*R* MDO polytype and (d,h) the disordered 14*H* LPSO phase. White and black arrows in (a-c, e-g) indicate the reciprocal lattice rows of the OD family reflections and the characteristic reflections, respectively. Transmitted beam and fundamental reflections for h.c.p. Mg are marked for references with circles and black triangles, respectively. The [$01\bar{1}l$]* and [$11\bar{2}l$]* reciprocal lattice rows in the SAED patterns for the disordered structure are marked with broken lines in (d, h).

Table 1. The OD groupoid symbols for the OD groupoid families generated by four different types of preferential block stacking of types A_1 to A_4 in the 14*H*-type Mg-Al-Gd LPSO phase and crystallographic parameters for MDO polytypes derived for each block stacking type.

Stacking type	OD groupoid symbol	Space group for the MDO polytype	Ramsdell notation for the MDO polytype	Lattice parameters for the MDO polytype
A_1	Not applicable (fully ordered structure)	$P6_3/mcm$ (#193)	2*H*	$a = b = 1.12$ nm, $c = 3.72$ nm $\alpha = \beta = 90°$, $\gamma = 120°$
A_2	$P \quad 1 \quad 1 \quad 1 \quad \left(\bar{3}\right) \quad \frac{2}{m} \quad \frac{2}{m} \quad \frac{2}{m}$ $\left\{ \frac{2_1}{n_{1/3,2}} \quad \frac{2}{n_{-2/3,2}} \quad \frac{2_{-1}}{n_{1/3,2}} \quad \begin{pmatrix} \bar{6} \\ 2_2 \\ 6_6 \\ n_{1,1/3} \end{pmatrix} \quad 1 \quad 1 \quad 1 \right\}$	$P6_322$ (#182)	2*H*	$a = b = 1.12$ nm, $c = 3.72$ nm $\alpha = \beta = 90°$, $\gamma = 120°$
		$R\bar{3}c$ (#167)	6*R*	$a = b = 1.12$ nm, $c = 11.16$ nm $\alpha = \beta = 90°$, $\gamma = 120°$
A_3	$P \quad 1 \quad 1 \quad 1 \quad \left(\bar{3}\right) \quad \frac{2}{m} \quad \frac{2}{m} \quad \frac{2}{m}$ $\left\{ \frac{2_{1/2}}{n_{1/2,2}} \quad \frac{2_{1/2}}{n_{-1/2,2}} \quad \frac{2_{-1}}{c_2} \quad \begin{pmatrix} \bar{6} \\ 2_2 \\ 6_6 \\ n_{1/2,1/2} \end{pmatrix} \quad 1 \quad 1 \quad 1 \right\}$	*Cmce* (#64)	2*O*	$a = 1.12$ nm, $b = \sqrt{3}a$, $c = 3.72$ nm $\alpha = \beta = \gamma = 90°$
		$P6_122$ (#178) $P6_522$ (#179)	6*H*	$a = b = 1.12$ nm, $c = 11.16$ nm $\alpha = \beta = 90°$, $\gamma = 120°$
A_4	$P \quad 1 \quad 1 \quad 1 \quad \left(\bar{3}\right) \quad \frac{2}{m} \quad \frac{2}{m} \quad \frac{2}{m}$ $\left\{ \frac{2_{1/2}}{n_{1/6,2}} \quad \frac{2}{n_{-1/3,2}} \quad \frac{2_{-1/2}}{n_{1/6,2}} \quad \begin{pmatrix} \bar{6} \\ 2_2 \\ 6_6 \\ n_{1/2,1/6} \end{pmatrix} \quad 1 \quad 1 \quad 1 \right\}$	$C222_1$ (#20)	2*O*	$a = b = 1.12$ nm, $c = 3.72$ nm $\alpha = \beta = \gamma = 90°$
		$C2/c$ (#15)	$2M_1$	$a = \sqrt{3}b$, $b = 1.12$ nm, $c = 3.23$ nm $\alpha = 90°$, $\beta = 101.56°$, $\gamma = 90°$
		Cc (#9)	$2M_2$	$a = \sqrt{3}b$, $b = 1.12$ nm, $c = 3.18$ nm $\alpha = 90°$, $\beta = 95.84°$, $\gamma = 90°$
		$P6_122$ (#178) $P6_522$ (#179)	6*H*	$a = b = 1.12$ nm, $c = 11.16$ nm $\alpha = \beta = 90°$, $\gamma = 120°$

Table 2. The OD groupoid symbols for the OD groupoid families generated by three different types of preferential block stacking of types C_1 to C_3 in the 18*R*-type Mg-Al-Gd LPSO phase described in [18] and crystallographic parameters for MDO polytypes derived for each of the OD groupoid families.

Stacking type	OD groupoid symbol	Space group for the MDO polytype	Ramsdell notation for the MDO polytype	Lattice parameters for the MDO polytype
C_1	$P \quad 1 \quad 1 \quad 1 \quad \left(\bar{3}\right) \quad \frac{2}{m} \quad \frac{2}{m} \quad \frac{2}{m}$ $\left\{ 1 \quad 1 \quad 1 \quad \begin{pmatrix} \bar{3} \\ 3_3 \end{pmatrix} \quad \frac{2_{1/3}}{n_{1/3,2}} \quad \frac{2_{-1/3}}{n_{1/3,2}} \quad \frac{2}{n_{-2/3,2}} \right\}$	$C2/m$ (#12)	1*M*	$a = 1.12$ nm, $b = \sqrt{3}a$, $c = 1.62$ nm $\alpha = 90°$, $\beta = 103.29°$, $\gamma = 90°$
		$C2/c$ (#15)	2*M*	$a = 1.12$ nm, $b = \sqrt{3}a$, $c = 3.18$ nm $\alpha = 90°$, $\beta = 96.74°$, $\gamma = 90°$
		$P3_112$ (#151) $P3_212$ (#153)	3*T*	$a = b = 1.12$ nm, $c = 4.74$ nm $\alpha = \beta = 90°$, $\gamma = 120°$
C_2	$P \quad 1 \quad 1 \quad 1 \quad \left(\bar{3}\right) \quad \frac{2}{m} \quad \frac{2}{m} \quad \frac{2}{m}$ $\left\{ 1 \quad 1 \quad 1 \quad \begin{pmatrix} \bar{3} \\ 3_3 \end{pmatrix} \quad \frac{2}{n_{1/3,2}} \quad \frac{2_{-1/6}}{n_{-1/6,2}} \quad \frac{2_{1/6}}{n_{-1/6,2}} \right\}$	$C2/m$ (#12)	1*M*	$a = 1.12$ nm, $b = \sqrt{3}a$, $c = 1.59$ nm $\alpha = 90°$, $\beta = 96.74°$, $\gamma = 90°$
		$C2/c$ (#15)	2*M*	$a = 1.12$ nm, $b = \sqrt{3}a$, $c = 3.17$ nm $\alpha = 90°$, $\beta = 93.38°$, $\gamma = 90°$
		$P3_112$ (#151) $P3_212$ (#153)	3*T*	$a = b = 1.12$ nm, $c = 4.74$ nm $\alpha = \beta = 90°$, $\gamma = 120°$
C_3	$P \quad 1 \quad 1 \quad 1 \quad \left(\bar{3}\right) \quad \frac{2}{m} \quad \frac{2}{m} \quad \frac{2}{m}$ $\left\{ 1 \quad 1 \quad 1 \quad \begin{pmatrix} \bar{3} \\ 3_3 \end{pmatrix} \quad \frac{2_{1/6}}{n_{5/6,2}} \quad \frac{2_{-1/2}}{n_{-1/6,2}} \quad \frac{2_{1/3}}{n_{-2/3,2}} \right\}$	$P\bar{1}$ (#2)	1A	$a = b = 1.12$ nm, $c = 1.66$ nm $\alpha = 93.23°$, $\beta = 106.37°$, $\gamma = 120°$
		$C2/c$ (#15)	$2M_1$	$a = 1.12$ nm, $b = \sqrt{3}a$, $c = 3.29$ nm $\alpha = 90°$, $\beta = 106.45°$, $\gamma = 90°$
		$C2/c$ (#15)	$2M_2$	$a = 1.12$ nm, $b = \sqrt{3}a$, $c = 3.25$ nm $\alpha = 90°$, $\beta = 103.29°$, $\gamma = 90°$
		$C2/c$ (#15)	$2M_3$	$a = 1.12$ nm, $b = \sqrt{3}a$, $c = 3.17$ nm $\alpha = 90°$, $\beta = 93.38°$, $\gamma = 90°$
		$P3_1$ (#144) $P3_2$ (#145)	3*T*	$a = b = 1.12$ nm, $c = 4.74$ nm $\alpha = \beta = 90°$, $\gamma = 120°$